

Formation-Damage Evaluation From Nonlinear Skin Growth During Coreflooding

P. Bedrikovetsky, SPE, University of Adelaide, A.S.L. Vaz Jr., North Fluminense State University, and C. Furtado and A.L.S. de Souza, Petrobras/CENPES

Summary

Injectivity decline of oilfield injection wells is a widespread phenomenon during seawater/produced-water injection. The decline may result in significant cost increase of the waterflooding project. Reliable modeling-based prediction of injectivity-index decrease is important for waterflood design as well as for the planning of preventive injected-water treatment. One of the reasons for well injectivity decline is permeability decrease caused by rock plugging by solid/liquid particles suspended in the injected water.

The mathematical model for deep-bed filtration contains two empirical functions: the filtration coefficient and the formation-damage coefficient. These empirical coefficients must be determined from laboratory coreflood tests by forcing water with particles to flow through the core samples. A routine laboratory method determines the filtration coefficient from expensive and difficult particle-concentration measurements at the core effluent; then, the formation-damage coefficient is determined from inexpensive and simple pressure-drop measurements. An alternative three-point-pressure method uses pressure data at an intermediate point of the core, supplementing pressure measurements at the core inlet and outlet. The method provides unique and stable values for constant-filtration and formation-damage coefficients.

In the current work, we consider a more complex case in which both coefficients are linear functions of retained-particle concentration. In this case, the model is fully determined by four constants. The three-point-pressure method furnishes unique values for the four model parameters. A new semianalytical model for axisymmetric suspension filtration was developed to predict well-injectivity decline from the linear coreflood data with pressure measurements in three core points.

Introduction

Produced-water reinjection (PWRI) and seawater injection during waterflood projects may result in dramatic injectivity decline. The phenomenon was widely reported for North Sea, Gulf of Mexico, and Campos basin oil fields. One of the main reasons for injectivity impairment is the solid and oily particles captured from the injected water by the rock, causing steep permeability decline (Todd et al. 1979; Nabzar et al. 1996; Pang and Sharma 1997; Chauveteau et al. 1998). The reliable injectivity-decline prediction—allowing for injector-stimulation planning and for the choice of optimal water-management strategy—is based on mathematical modeling with well-known values of the model coefficients.

The classical mathematical model for deep-bed filtration, presented by Herzig et al. (1970), Sharma and Yortsos (1987), and Rousseau et al. (2007), contains two empirical functions: the filtration coefficient that is equal to particle-capture probability per unit length of its trajectory and the formation-damage coefficient that reflects permeability decrease caused by particle retention (the mathematical model for deep-bed filtration, described further in the text, contains equations for both coefficients); both coefficients are functions of the retained-particle concentration. Knowledge of these two parameters is essential for predicting well-injectivity

decline during seawater/produced-water injection. Certain existing software packages for predicting well-injectivity losses provide the option of adjusting the pressure-drop curve by matching both parameters.

The filtration and formation-damage coefficients are empirical parameters. Despite this, these parameters can be calculated theoretically for simplified pore-space models; for the case of a natural rock, they must be determined from laboratory coreflood tests by flowing water with particles through the rock. Works by Pang and Sharma (1997) and Wennberg and Sharma (1997) show that both parameters can be inferred from combined measurements of core-pressure drop and of suspended-particle concentration in the core outlet water.

Usually, a coreflood test is accompanied by pressure-drop measurements. These measurements are inexpensive and simple to perform, and, therefore, they are widespread in the literature. Nevertheless, suspended-particle-concentration data in the core-outlet water during laboratory tests are hardly available in the literature [see for example such widely referred to studies as van Oort et al. (1993), Ali et al. (2005), and Al-Abduwani (2005)]. This is because the measurements of concentration data require special equipment, and the measurements are cumbersome if compared with the measurements of the pressure drop (Al-Abduwani 2005; Tiab and Donaldson 1996). The afore-mentioned difficulties are the motivation for attempting to determine the filtration and formation-damage coefficients from pressure measurements only.

The constant filtration and formation damage coefficients can be calculated from the pressure measurements at an intermediate point of the core as well as at the core entrance and exit during the deep-bed-filtration coreflood (so-called three-point-pressure method) (Bedrikovetsky et al. 2001, 2003). The method provides unique values for two constant coefficients; the solution is stable with respect to small perturbations of the measured pressure histories.

The pressure drop on the overall core or on its first section grows linearly with time for the case of constant filtration and formation-damage coefficients (Pang and Sharma 1997). Nevertheless, numerous laboratory tests show that the pressure drop can grow nonlinearly with time [see Todd et al. (1979), Al-Abduwani (2005), Todd et al. (1984), Moghadasi et al. (2004)]. It requires application of a more complex deep-bed-filtration model.

In the present work, the three-point-pressure method is extended for the case in which the filtration and formation-damage coefficients are linear functions of retention concentration. It provides nonlinear pressure-drop rise with time. Changing the filtration and formation-damage coefficients from constant to linear functions of retention concentration results in an increase of the number of model constant parameters from two to four. The four model parameters can be calculated from nonlinear curves of pressure drops across the core and across its first section, which are measured during deep-bed-filtration flooding of homogeneous cores. A new semianalytical model for axisymmetric suspension flow with linear filtration and formation-damage functions has been derived, allowing prediction of the injectivity-index decline.

The structure of the text is as follows. First, the classical equations for deep-bed filtration are presented, and two empirical functions—those for filtration and for formation damage—are introduced. Then the inverse problem for determination of the two functions from the coreflood data is formulated. Further, a

Copyright © 2011 Society of Petroleum Engineers

This paper (SPE 112509) was accepted for presentation at the SPE International Symposium and Exhibition on Formation Damage Control, Lafayette, Louisiana, USA, 13–15 February 2008, and revised for publication. Original manuscript received for review 14 November 2007. Revised manuscript received for review 18 May 2010. Paper peer approved 12 October 2010.

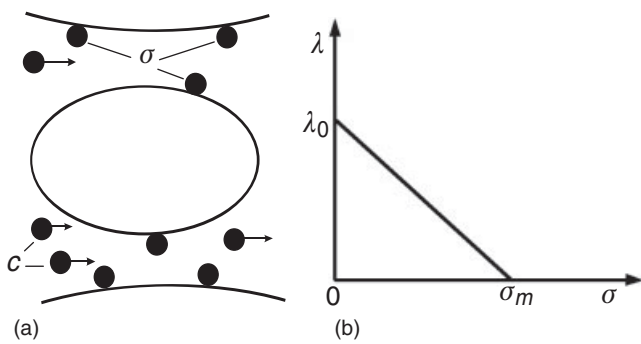


Fig. 1—Retention conditions for Langmuir filtration function; (a) filtration rate is proportional to vacancy concentration; (b) constants λ_0 and σ_m for linear filtration function.

semianalytical model for the case under consideration is presented, and the method for determination of four model constants from two curves of pressure-drop rise on the overall core and on its first section is developed. Application of the proposed method for the treatment of two data sets of laboratory tests is also presented. At the end of the paper we show how the obtained values for four injectivity-damage parameters are applied for well-injectivity prediction.

Mathematical Model for Deep-Bed Filtration

During seawater injection, mainly solid particles penetrate into the reservoir; their retention in rock results in permeability decline and in consequent decrease of well injectivity index. Oily water is injected during PWRI, also resulting in injectivity impairment. Oily and solid particles are deposited in the rock with different rates (Ali et al. 2007, 2009; Soo and Radke 1986a, 1986b). They interact during suspension transport in porous media, forming relatively large aggregates. Also, the particles can flocculate at some values of brine salinities and pH. These processes are ignored in the current work in which the so-called classical deep-bed-filtration model (Pang and Sharma 1997; Chauveteau et al. 1998; Herzig et al. 1970; Sharma and Yortsos 1987; Rousseau et al. 2007; Wennberg and Sharma 1997) is used.

Deep-bed filtration with similar modeling challenges occurs during drilling-fluid invasion into the formation with consequent permeability damage (Bailey et al. 2000; Suryanarayana et al. 2007; Tang et al. 2005). It also occurs in fines migration causing productivity decline (Zang and Dusseault 2004; Miranda and Underdown 1993), in injectivity decline of fractured wells (Mojarad and Settari 2005; Bachman et al. 2003; Settari 1985), and in waste disposal in aquifers (Harding et al. 2002, 2003).

Following previous work (Pang and Sharma 1997; Chauveteau et al. 1998; Herzig et al. 1970; Sharma and Yortsos 1987; Rousseau et al. 2007; Wennberg and Sharma 1997), we briefly describe the mathematical model for flow of suspensions in porous media.

Let us introduce the overall suspended- and retained-particles concentrations. **Fig. 1** shows suspension concentration c of moving particles and concentration σ of particles attached to grain surfaces. Both concentrations are volumetric. Suspension concentration c is defined as a particle volume contained in a unit volume of the carrier fluid (per unit volume of the porous space). Retained concentration σ is equal to the volume of particles captured by a unit volume of the rock.

Conservation of suspended and retained particles in porous media is given by

$$\phi \frac{\partial c}{\partial t} + U \frac{\partial c}{\partial x} = - \frac{\partial \sigma}{\partial t}, \quad (1)$$

where U is the flow velocity.

It is assumed that water is incompressible, and particle retention by rock does not change the total volume of the system “water particles.” It results in conservation of suspension flux, $U(t)$. Porosity ϕ in Eq. 1 is constant for homogeneous core. The

suspension density and viscosity are assumed to be constant for diluted suspensions. Diffusion is neglected.

It is assumed that the retention rate is proportional to particle advective flux cU . The proportionality coefficient λ depends on retained concentration σ and is called the filtration function, $\lambda(\sigma)$. The retention rate is also proportional to the number of vacancies. If A is a specific rock surface and b is an “individual” area on grain surface filled by one retained particle, the vacancy concentration is proportional to the free grain surface, which is equal to $A - b\sigma$ (Fig. 1a).

Finally, the retention rate is proportional to the product

$$(A - b\sigma)cU. \quad (2)$$

Introducing the proportionality coefficient yields the equation for retention rate:

$$\frac{\partial \sigma}{\partial t} = \lambda_0 \left(1 - \frac{\sigma}{\sigma_m} \right) cU. \quad (3)$$

The filtration function in Eq. 3 is linear with respect to retention concentration (Fig. 1b):

$$\lambda(\sigma) = \lambda_0 \left(1 - \frac{\sigma}{\sigma_m} \right). \quad (4)$$

If linear dependency (Eq. 4) for $\lambda(\sigma)$ holds for the whole interval of retention-concentration variation, the maximum of retention concentration σ_m corresponds to the case where the overall vacant grain surface is filled by particles (i.e., σ_m is proportional to the initial number of vacancies). If $\lambda(\sigma)$ is linear just for some initial interval of σ and becomes nonlinear for larger values of retained concentration, σ_m can be interpreted just as a phenomenological coefficient in an equation for a straight line without any specific physical meaning. If the retention concentration is negligibly smaller than the initial concentration of vacancies, the retained particles do not affect the vacancy concentration, they do not change the retention conditions, and the filtration function is constant. Formally, it corresponds to infinite value of the maximum retention concentration σ_m .

So, the retention rate is characterized by two constants: by the initial filtration coefficient λ_0 and by the maximum retention concentration σ_m . Parameters λ_0 and σ_m depend on salinity and pH of the injected water, on the mineral grain-surface composition, on the particle size and particle wettability, on the temperature and on other factors (i.e., two constants are determined by the rock and the injected-fluid properties).

So-called collective effects of particle interaction at high concentrations lead to nonlinear filtration coefficient $\lambda = \lambda(\sigma)$. Its form also depends on such factors as brine salinity and pH electric Derjagin-Landau-Verwey-Overbeek (DLVO) forces [numerous examples with other references can be found in the literature (Nabzar et al. 1996; Chauveteau et al. 1998; Tiab and Donaldson 1996)].

Particle retention results in permeability decrease (i.e., the permeability is σ -dependent):

$$U = - \frac{k(\sigma)}{\mu} \frac{\partial p}{\partial x}. \quad (5)$$

The permeability dependence of retained concentration $k(\sigma)$ is called the formation-damage function. Different empirical formulae for $k(\sigma)$ have been proposed in the literature (Bailey et al. 2000; Al-Abduwani et al. 2005; Nabzar et al. 2005; Bedrikovetsky 1993). Usually, the hyperbolic form

$$k(\sigma) = \frac{k(0)}{1 + \beta\sigma + \beta_2\sigma^2} \quad (6)$$

with $\beta_2 = 0$ is used, where β is called the formation-damage coefficient.

The quadratic form of Eq. 6 with nonzero β_2 is used in previous work (Al-Abduwani 2005; Al-Abduwani et al. 2005) to adjust coreflood injectivity-impairment data. Eq. 6 corresponds to the linear function of formation-damage coefficient β vs. retention concentration σ . Further in the text, β_2 is called the second formation-damage coefficient.

The coefficients β and β_2 are empirical constants characterizing formation damage; they depend on the rock properties and on the injected-suspension properties.

The system (Eqs. 1 and 3) consists of two equations for two unknowns, c and σ . For the injection of constant-concentration suspension into a clean bed, the system of governing equations is subject to the boundary condition of given injected concentration c^0 at the core inlet $x=0$ and zero initial condition for suspended and retained concentrations at $t=0$.

Several analytical solutions of the problem (Eqs. 1 and 3) have been reported in the literature (Herzig et al. 1970). The analytical solution for the clean-bed injection problem for the case of constant filtration and formation-damage coefficients is presented in Appendix A.

While the initial-boundary problem is solved, pressure distribution along the core during flooding can be found from Eqs. 5 and 6 by direct integration of pressure gradient in x from zero to L .

Formulation of the Problem

Deep-bed filtration with injection of seawater or PWRI under reservoir conditions is described by a 3D system (Eqs. 1 through 6) with the zero initial conditions in the geometry of streamlines near the injection well. Streamline geometries for fractured (Mojarad and Settari 2005; Bachman et al. 2003; Settari 1985), horizontal (Suryanarayana et al. 2007; Harding et al. 2002), and perforated (Tang et al. 2005) injectors differ significantly from the linear-parallel coreflood flow. The 3D system contains the same empirical functions as the system (Eqs. 1 through 6) does [i.e., the model parameters are the filtration function $\lambda(\sigma)$ and the formation-damage function $k(\sigma)$]. The functions depend on rock and injected-fluid properties and are different for different field conditions. They can be predicted theoretically only for some simplified particular cases (Bedrikovetsky 1993; Civan 2007).

Particle-deposition profile during coreflood is inhomogeneous, since the retention concentration decreases along the core. Therefore, the functions $\lambda(\sigma)$ and $k(\sigma)$ cannot be measured directly during coreflood. They can be determined from the coreflood data by solution of inverse problems.

The filtration coefficient is a kinematics property of the filtration system, and it should be determined from kinetics of particle capture. Usually $\lambda(\sigma)$ is determined from breakthrough concentration (Alvarez et al. 2006a); see Fig. 2. The solution of the inverse problem always exists, is unique, and is stable with respect to small perturbations of effluent concentration. If the filtration function is already known, the formation-damage function $k(\sigma)$ can be determined from pressure drop on the core as measured during the coreflood (Fig. 2). The solution of this inverse problem also always exists, is unique, and is stable with respect to small perturbations of pressure-drop history (Alvarez et al. 2006b).

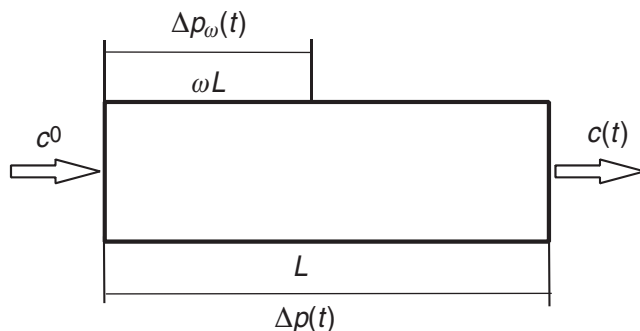


Fig. 2—Schema of three-point-pressure injectivity coreflood test.

Consider the case of constant filtration and formation damage coefficients. The solution (Eq. A-1) shows that the breakthrough concentration $c(L, t)$ is constant. It allows calculation of filtration coefficient λ_0 from the breakthrough concentration (Pang and Sharma 1997; Wennberg and Sharma 1997):

$$\lambda_0 = \frac{1}{L} \ln \left[\frac{c^0}{c(L, t)} \right] \quad \dots \dots \dots (7)$$

Usually corefloods are performed under the constant rate U . In this case, dimensionless pressure drop is called the impedance and is determined as

$$J(t) = \frac{\Delta p(t)}{\Delta p(0)} \quad \dots \dots \dots (8)$$

Impedance increases because of accumulation of the deposit and is caused by consequent increase in permeability damage.

For the case of constant filtration and formation-damage coefficients, the impedance is a linear function of time, and the proportionality coefficient m is a function of filtration and formation-damage coefficients (Eqs. A-3 and A-4). So, the pressure-drop measurements allow calculating the impedance slope m and determining the formation-damage coefficient:

$$\beta = \frac{m}{\phi c^0 (1 - e^{-\lambda_0 L})} \quad \dots \dots \dots (9)$$

Laboratory determination of pressure drop is a simple and inexpensive routine procedure requiring pressure transducers along with the pump. Concentration measurement is a cumbersome procedure requiring expensive and often unreliable particle counters.

Constant filtration and formation-damage coefficients can be determined from pressure measured at core inlet, core outlet, and at some intermediate core point [the detailed derivations can be found in Bedrikovetsky et al. (2001, 2003)] (Fig. 2). Two impedance slopes m and m_ω are calculated from pressure drops across the core and across its first section, respectively. Appendix A shows that from the formulae for impedance slopes (Eqs. A-4 and A-5) follows the transcendental equation (Eq. A-7) for unknown y . Fig. 3 presents plots of the left- and right-hand sides of Eq. A-7. Since $\omega < 1$, the plot of the left-hand side y^ω is a convex function. The left-hand side is a linear function of y . The convex curve in Fig. 3 is denoted as 2; straight line is denoted as 1.

It follows from Eqs. A-4 and A-5 that $m_\omega/m < 1$. Therefore, a straight line always intersects the curve in a single point (Fig. 3).

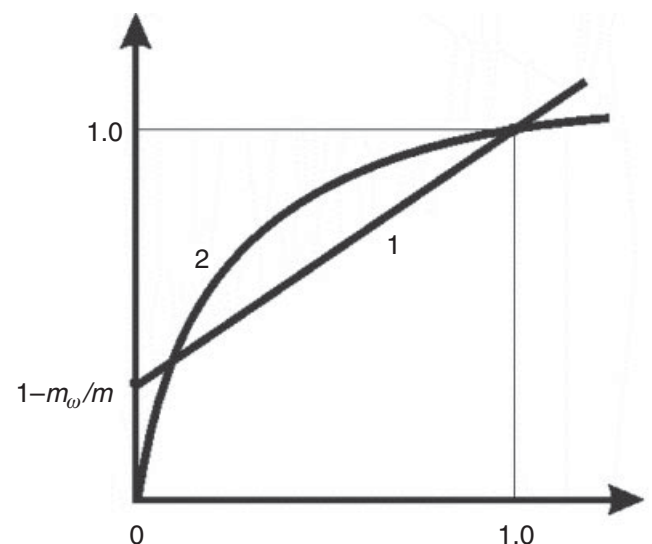


Fig. 3—Graphical method to determine constant filtration and formation-damage coefficients.

There is a unique root of the transcendental equation (Eq. A-7). Therefore, the solution of the inverse problem of determination of filtration coefficient from pressure measurements in three core points does exist and is unique.

Several cases of nonlinear pressure-drop increase during seawater coreflooding have been presented in the literature (Todd et al. 1979; Al-Abduwani 2005; Todd et al. 1984; Moghadasi et al. 2004). Consider a nonlinear pressure-drop curve. While the impedance curve has one degree of freedom for the case of constant filtration and formation-damage coefficients, expressed by parameter m in Eq. A-3, a nonlinear curve has at least two degrees of freedom. Thus, two impedance curves, as measured on the overall core and on its first section, have at least four degrees of freedom.

The system of deep-bed filtration, in which filtration and formation-damage coefficients are linear functions of retention concentration σ , also has four degrees of freedom—it contains four independent empirical constants, λ_0 , σ_m , β , and β_2 . In the next two sections of the paper, we determine the four injectivity-damage constants from two impedance curves for the overall core and for its first section, allowing characterization of the deep-bed-filtration system with filtration and formation-damage coefficients as linear functions of retained concentration from three pressure measurements along the homogeneous core.

Semianalytical Model for Deep-Bed Filtration With Linear Filtration and Formation-Damage Coefficients

A 1D deep-bed-filtration problem (Eqs. 1 and 3) for linear filtration function (Eq. 4) allows for an exact analytical solution [see Soo and Radke (1986a, 1986b)] where suspended and retained concentrations are given by explicit formulae:

$$c(x,t) = c^0 \left[1 + e^{-\frac{\lambda_0 c^0}{\sigma_m} (Ut - \phi x)} (e^{\lambda_0 x} - 1) \right]^{-1} \quad \dots \dots \dots (10)$$

$$\sigma(x,t) = \sigma_m \frac{e^{\frac{\lambda_0 c^0}{\sigma_m} (Ut - \phi x)} - 1}{e^{(\lambda_0 x)} + e^{\frac{\lambda_0 c^0}{\sigma_m} (Ut - \phi x)} - 1} \quad \dots \dots \dots (11)$$

Expressing the pressure gradient from Eq. 5 and integrating it in x , one obtains an expression for the pressure drop on the overall core and calculates impedance:

$$J(t) = 1 + \frac{\beta}{L} \int_0^L \sigma(x,t) dx + \frac{\beta_2}{L} \int_0^L \sigma^2(x,t) dx. \quad \dots \dots \dots (12)$$

Formula for impedance variation during coreflooding on the first core section $J_{\omega}(t)$ is obtained from Eq. 12 by changing from L to ωL , where ωL is the length of the first core section (Fig. 2). As mentioned before, two curves $J(t)$ and $J_{\omega}(t)$ have at least four degrees of freedom, allowing for determination of four model constants.

The proposed method for treatment of two nonlinear impedance curves, as measured on the overall core and on its first section, determines the constants λ_0 , σ_m , β , and β_2 by the least-squares method:

$$\min_{(\lambda_0, \sigma_m, \beta, \beta_2)} \left\{ \sum_{i=1}^n [J(t_i, \lambda_0, \sigma_m, \beta, \beta_2) - J_i]^2 + \sum_{k=1}^l [J_{\omega}(t_k, \lambda_0, \sigma_m, \beta, \beta_2) - J_{\omega k}]^2 \right\} \quad \dots \dots (13)$$

Here, the impedance values $J(t_i, \lambda_0, \sigma_m, \beta, \beta_2)$ are calculated by Eq. 12 for the given values of four constants. The values J_i correspond to pressure-drop measurements during the coreflood at moments t_i . The impedance values of $J_{\omega}(t_k, \lambda_0, \sigma_m, \beta, \beta_2)$ and $J_{\omega k}$ are the calculated and measured values for the first core section, respectively.

The optimization method (Eq. 13) of the solution of the inverse problem determines four model constants by minimizing the standard deviation of laboratory data from the modeling results.

Treatment of Laboratory Data

In the current section, the optimization technique (Eq. 13) is applied to determine four injectivity-damage parameters from pressure measured in three points of a homogeneous core. In each experiment, differential pressure was measured at multiple points along the porous medium during flow at a constant flow rate and constant injected-particle concentration. We determined the damage parameters λ_0 , σ_m , β , and β_2 by matching the overall ΔP and ΔP_{ω} at the first core section using Eqs. 12 and 13. To validate the method, we then used the parameters obtained to match the pressure response at the other pressure tap.

Suspension of solid aluminium oxide particles is injected in an artificial bed packed with spherical glass-bead grains (Moghadasi et al. 2004). Glass-bead diameter varies from 400 to 600 μm , with a median size of 480 μm . Bed permeability is 159 md, and porosity is 0.38. Particle diameter is 7 μm . Suspension concentration is 1,000 ppm. Flow rate in the first test is 25 cm^3/min . The tests are performed under standard conditions. Pressure is measured at core inlet, outlet, and in three intermediate points.

Fig. 4 shows impedance curves as obtained from pressure drop on the first, second, and third core sections and on the overall core (Curves 1, 2, 3, and 4, respectively). Coordinates of three intermediate pressure points correspond to $\omega=0.38$, 0.61, and 0.81 (i.e., to lengths of the first, second, and third sections, respectively).

The retention concentration decreases along the core, so average retention concentration in the first section is higher than that in the second section, average retention concentration in the second section is higher than that in the third section, and so on. Therefore, damage in the first section exceeds that in the second section, damage in the second section exceeds that in the third section, and so on. So, Curve 1 is located above Curve 2, then follows Curve 3, and then Curve 4.

Two impedance curves used for the model adjustment correspond to the first core section and to the overall core (Curves 1 and 4). The deviation of experimental points from the adjusted Curves 1 and 4 is small, allowing the claim that the laboratory and modeling data are in a good agreement.

Data treatment is performed by a nonlinear least-square method (Eq. 13); solution of the inverse problem was obtained using the optimization procedure. The Levenberg-Marquardt optimization algorithm was applied using the software MatLab. The initial points for the iterative optimization algorithm were obtained by linearization of the curves $J(t)$ and $J_{\omega}(t)$ and obtaining values of λ_0 and β by the three-point-pressure method (Bedrikovetsky et al. 2001, 2003).

The values of constant filtration and formation-damage coefficients have been determined from the coreflood and well-history data using different methods (Pang and Sharma 1997; Wennberg and Sharma 1997; Bedrikovetsky et al. 2001, 2003). Depending on pore and particle sizes and water composition, the filtration coefficient usually varies from 1 to 200 1/m. The formation-damage coefficient for different pore-space geometries and particle sizes varies from 1 to 1,000. The values of coefficients λ_0 and β , as presented in Table 1, vary within these intervals.

Fig. 4 also presents the impedance growth on the second and third sections. These data can be used to validate the model (Eqs. 1 through 6) and the method (Eq. 13) for the permeability-impairment system characterization. Assuming that the porous media are homogeneous, one concludes that the four damage parameters are constant along the core. So, the impedance curves for the second and third sections can be calculated for the values of damage parameters obtained from the first and fourth curves.

Fig. 4 exhibits a good match between the predicted and measured values, which validates the model (Eqs. 1 through 6).

Results of the second test for higher injection rate (50 cm^3/min) are presented in Fig. 5. The first curve is located above the second curve, the second curve lies above the third curve, and the third

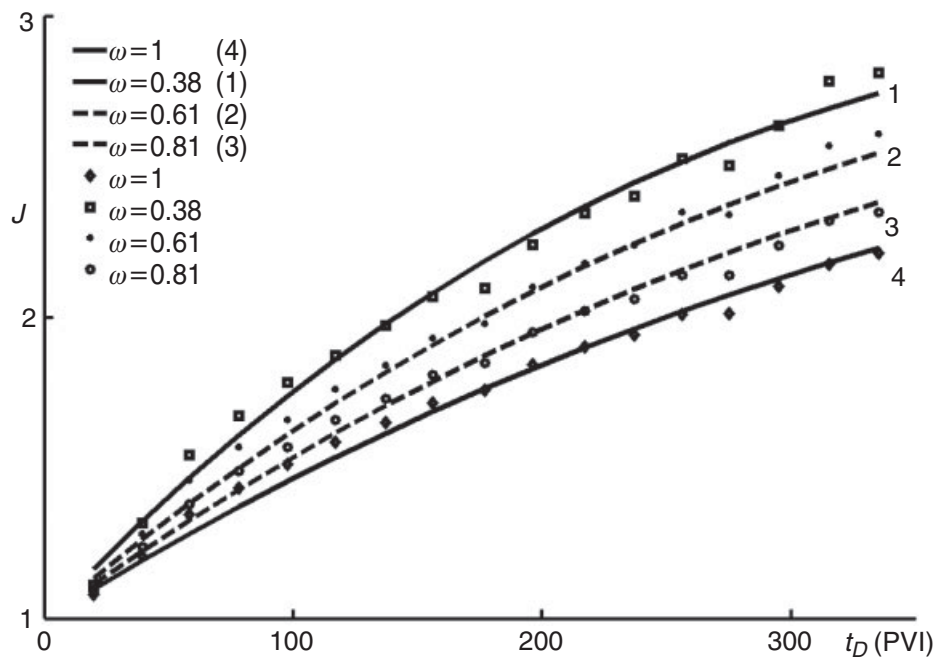


Fig. 4—Treatment of nonlinear pressure-drop curves for artificial cores (Moghadasi et al. 2004). PVI is pore volumes injected.

curve lies above the fourth curve because of a decrease in the retention profile along the core. The damage parameters, as obtained from the adjustment of Curves 1 and 4, are presented in Table 1. The values of filtration and formation-damage coefficients vary in the usual range (Pang and Sharma 1997; Wennberg and Sharma 1997; Bedrikovskiy et al. 2001, 2003). Curves 2 and 3 (predicted impedance) match well with the data measured on the second and third core sections.

Visually, the curves in Fig. 5 are almost straight lines. According to the analytical model (Eqs. A-1 and A-2), this corresponds to constant filtration and formation-damage coefficients (see Appendix A). The case of constant filtration and formation-damage coefficients is a particular case of the linear functions Eqs. 4 and 6, where $\beta_2=0$ and σ_m tends to infinity. Indeed, in Table 1, the value of β_2 for the second test is negligibly lower if compared with that obtained from the first test. The value of σ_m in the second test greatly exceeds that from the first test.

The laboratory coreflood with suspended solid particles in natural reservoir plugs was performed by Al-Abduwani (2005). Homogeneous Bentheimer sandstone from outcrops was used as a core material. Pressure was measured at the core inlet and outlet, and also in two intermediate points (Fig. 6). The superficial velocity was 2.9×10^{-3} m/s, concentration of injected hematite particles $c^0=11.5$ ppm, flooding duration is 12,131 seconds (1,017 PVI), core length $L=0.127$ m, permeability $k=1.46$ darcies, and porosity $\phi=0.22$. The data on the pressure drop across the first core section (Curve 1) and across the overall core (Curve 4) were used to tune the model by techniques (Eq. 13). One can observe a high-quality

match between the tuned and measured data (Curves 1 and 4). Then, pressure drop across the second and third sections was calculated and compared with the pressure-measurement data (Curves 2 and 3). The agreement between the modeled and measured Curve 3 is reasonable, while the deviation of the modeled Curve 2 from that measured is significant.

Todd et al. (1984) perform injection of a suspension with solid aluminium oxide particles into Clasach sandstone core (North Sea) with permeability of 582 md and porosity of 0.16. Particle size varies in the range of 3 to 5 μm . Medium pore-throat size is 25 μm . Injection rate is 108 cm^3/min . Suspension concentration is 5 ppm. Pressure is measured in four intermediate core points in addition to measurements at the core inlet and outlet, allowing selecting five core sections. The corresponding impedance curves are presented in Fig. 7. Owing to the decline of retention profile along the core, the experimental curves are located in order of impedance decline: 1, 2, 3, 4, 5.

The four damage parameters are determined by the adjustment of impedance curves on the first section and on the overall core (Curves 1 and 5, respectively) using the optimization technique (Eq. 13). The values presented in Table 1 vary in conventional ranges.

The obtained values of the four damage parameters are used to predict impedance curves for the second, third, and fourth core sections. The intermediate curves do not exhibit good match with measured data (Fig. 7). As reported in Todd et al. (1984), the core is not homogeneous; the relative variation of permeability along the core is 0.21. So, the damage coefficients also vary along the

TABLE 1—VALUES OF FOUR INJECTIVITY DAMAGE PARAMETERS AS OBTAINED FROM LABORATORY-DATA TREATMENT

Tests	Injectivity-Damage Parameters				Fit Quality	Prediction Quality
	β	β_2	$\lambda_0(1/\text{m})$	σ_m		
Mogadhasi et al. (2004) $V=25\text{ml/min}$	15	-28	5.6	0.64	0.0681	0.0966
Mogadhasi et al. (2004) $V=50\text{ml/min}$	4.4	-0.5	12	18.47	0.0190	0.0199
Al-Abduwani (2005)	130	1.5e5	29	0.18	0.0862	0.3097
Todd et al. (1979)	104	-1153	50	0.026	0.0667	0.7324

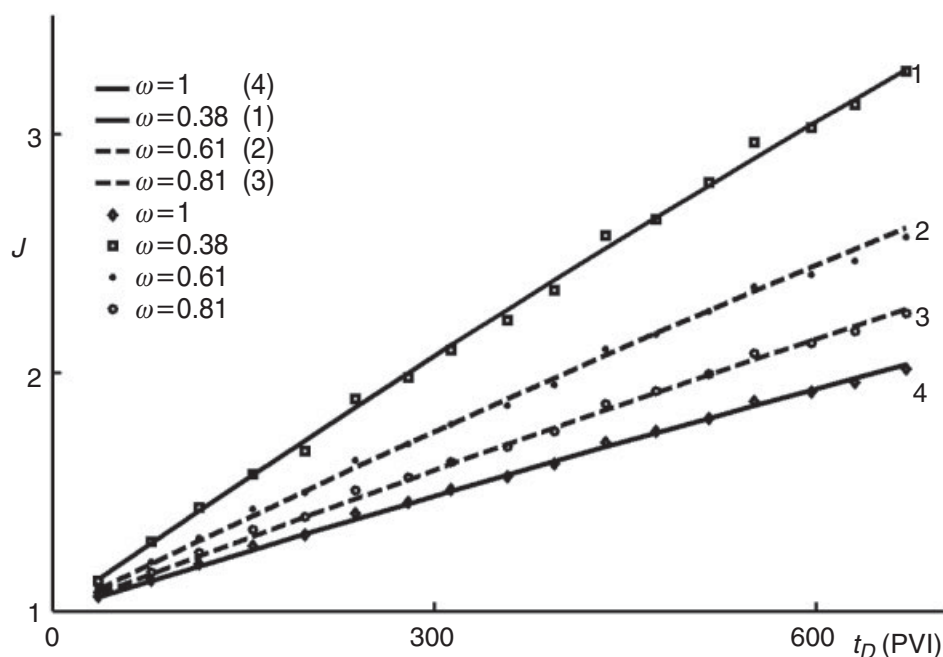


Fig. 5—Treatment of quasilinear pressure-drop curves (Moghadasi et al. 2004).

core, which explains deviation of predicted Curves 2, 3, and 4 from the measured data.

The standard deviation of the modeled curves from those measured is presented in Table 1. The column titled Fit Quality gives the deviation for the tuned curves, while the Prediction Quality column presents the deviation for the predicted curves. As observed from Figs. 4 through 7, the quality of tuning is high; the curves of the pressure drop across the first core section and across the overall core almost coincide with sequences of experimental points for all cases. The quality of prediction is lower than that of tuning. Very good prediction is observed for artificial cores (Figs. 4 and 5). A reasonable quality of predicted pressure drops across second and third core sections takes place for homogeneous Bentheimer core (Fig. 6). The standard deviation is the highest for flooding

the natural reservoir core (Fig. 7). This allows us to conclude that the lower the heterogeneity is, the higher the reliability is of the three-point-pressure method.

Nevertheless, validation of the three-point-pressure method for nonlinear deep-bed filtration in heterogeneous cores requires additional research. It is important to find out up to what value of the core heterogeneity index the proposed method is valid. Modeling of deep-bed filtration in composite cores could reveal the method sensitivity with respect to nonuniformity of the porosity and permeability. Yet, the correlations between the four damage parameters and permeability are not available in the literature. One way around the generation of four damage parameters for different rocks is micromodeling and upscaling of the damage parameters from the pore scale to the core scale, such as is performed in work

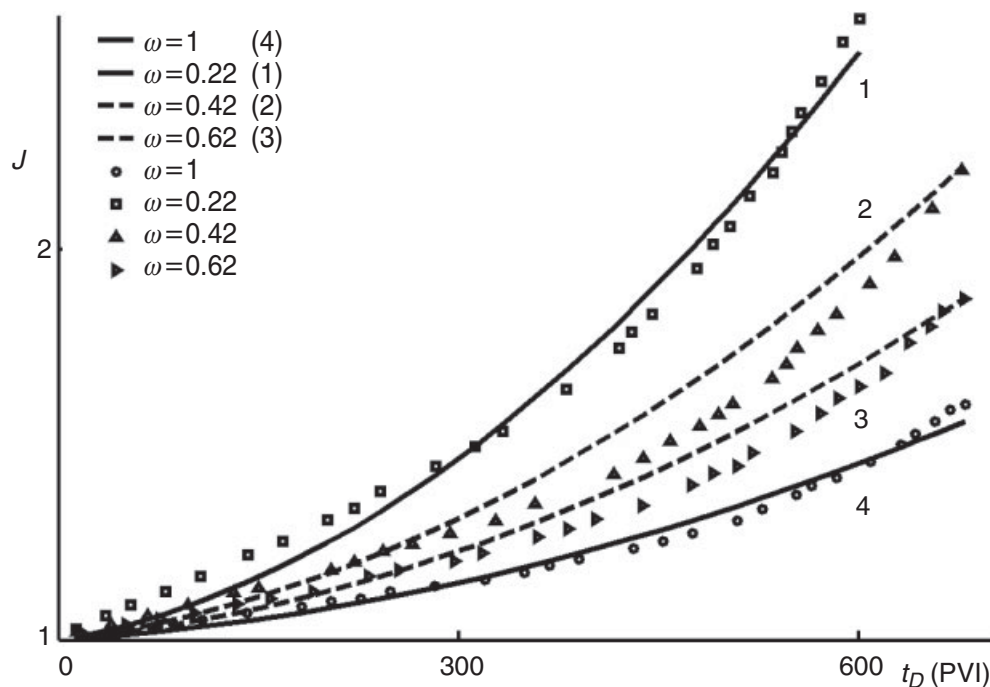


Fig. 6—Treatment of nonlinear pressure-drop curves for injection of hematite-particle suspension in Bentheimer core (Al-Abduni 2005).

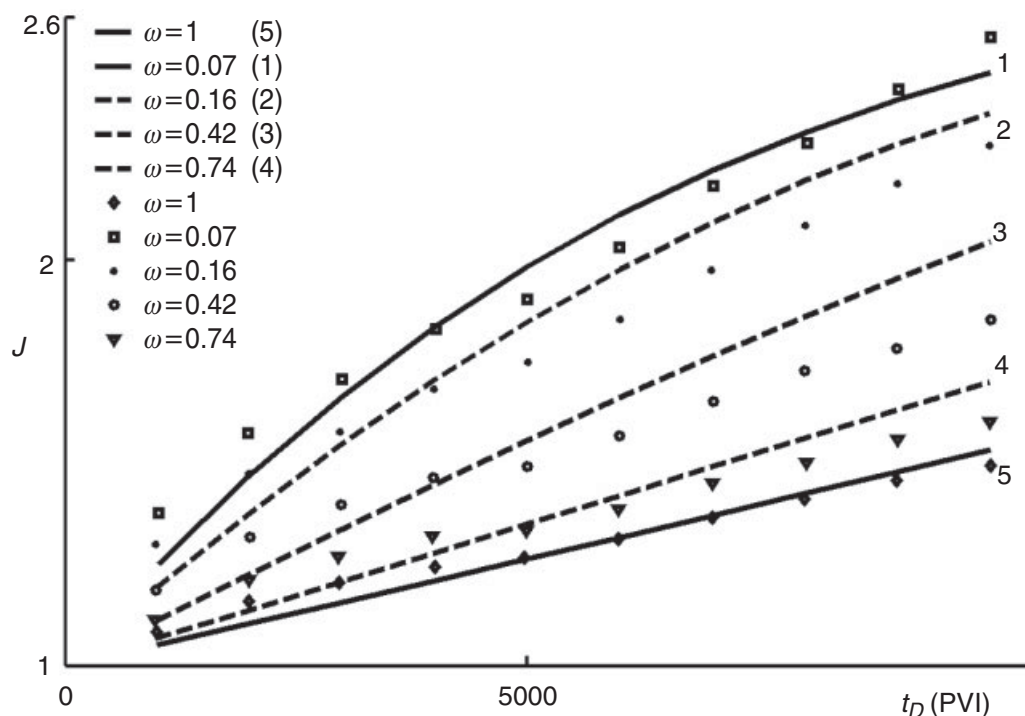


Fig. 7—Treatment of nonlinear pressure-drop curves for North Sea sandstone cores (Todd et al. 1984).

by Sharma and Yortsos (1987) and by Bedrikovetsky (2008). This research is outside of the scope of the current paper.

Estimates of Well Injectivity Index

Let us show how to use the values of four injectivity-damage parameters λ_0 , σ_m , β , and β_2 , as obtained by treatment of coreflood data, for well-injectivity decline prediction.

The model for vertical-well injectivity decline consists of nonlinear deep-bed-filtration equations for axi-symmetric flow geometry; see Eqs. B-1 through B-3. Exact semianalytical solution

of the radial deep-bed-filtration problem (Eqs. B-8 and B-9) allows calculating well impedance vs. time (Eq. B-10). Figs. 8 and 9 show well impedance growth during the injection. The basic-case data are typical for North Sea Clasach sandstones (Curves 4 and 2) (Todd et al. 1984); the values of four damage parameters are given in Figs. 8 and 9. Other curves correspond to perturbed values of the basic parameters.

Impedance curves almost stabilize with time (i.e., its time derivative tends to zero when time tends to infinity). The stabilization is explained by reaching the maximum retention concentration

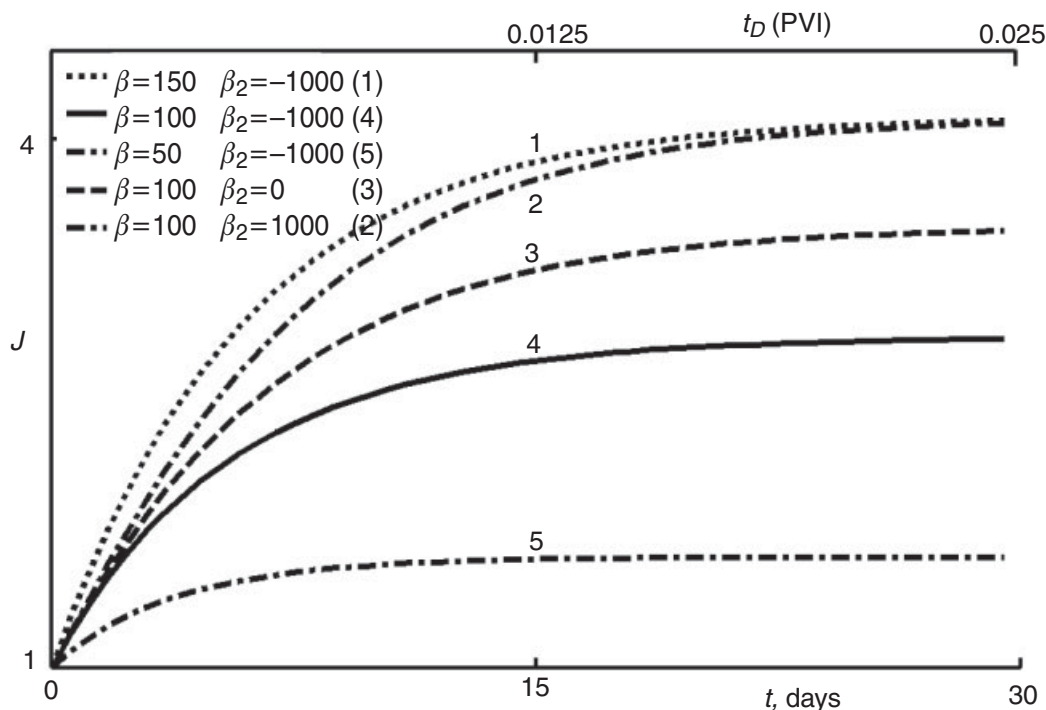


Fig. 8—Effect of two formation-damage coefficients β and β_2 on impedance curve: impedance vs. real time and PVI.

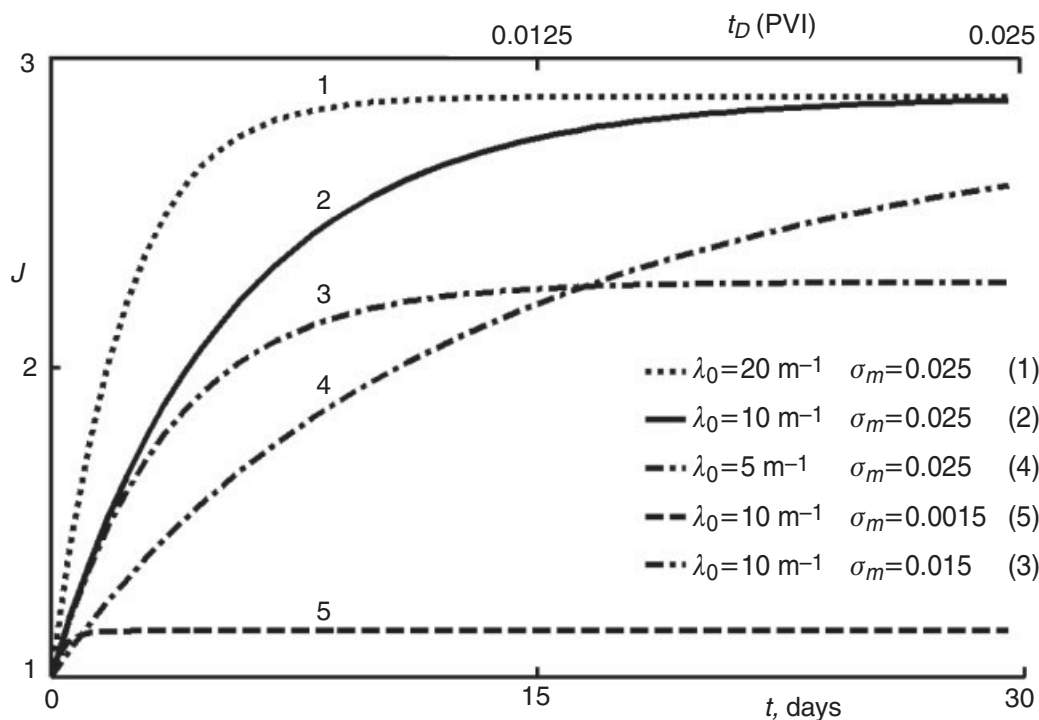


Fig. 9—Sensitivity of impedance curve to variation of filtration function: impedance vs. real time and PVI.

σ_m in each point around the well, so the particle capture by the rock no longer happens (see Eqs. 3 and 4). The higher the distance of a reservoir point is from the injector, the later the maximum retention concentration will be reached in this point.

In offshore waterflood operations, the injectivity-index stabilization at some reduced value happens quite often. The usual explanation of this phenomenon is well fracturing (Mojarad and Settari 2005; Bachman et al. 2003; Settari 1985). Injection of particulated suspension and particle capture by the rock lead to reduced permeability, forcing the wellbore pressure to increase to maintain the injection rate. The fracture opens because of high pressure near the damaged injector. It propagates deeper into the formation because of further permeability decline and increase of hydraulic resistivity during the injected-particle-suspension leakoff. Fracture propagation and increase of the injected surface compensate the hydraulic resistivity increase because of deep-bed filtration and external-filter-cake formation on the fracture walls.

Another explanation for injectivity-index stabilization is erosion of external and internal filter cakes, in which the pressure gradient increases because of permeability decline. The pressure gradient drags the dislodged particles from the cakes deep into the reservoir (Miranda and Underdown 1993).

Well injectivity was calculated for the typical conditions of North Sea field studies in the literature (Todd et al. 1979; Todd et al. 1984): drainage radius $R_c=500$ m, formation thickness $h=30$ m, injected rate 3180 m³/d, porosity $\phi=0.16$. The well impedance stabilizes at the value $J=2.85$ after 30 days (0.025 PVI) and almost does not grow further (solid curves in Figs 8 and 9). Strictly speaking, particle retention occurs during the overall injection period in the swept reservoir zones. Nevertheless, the larger the distance from the well, the lower the effect of deposition-induced permeability impairment in the reservoir point on injectivity index.

Fig. 8 shows sensitivity of the impedance curve with respect to variation of formation-damage coefficient (Curves 1 and 5) and of second formation damage coefficient (Curves 2 and 3). The “basic” Curve 4 corresponds to typical values of adjustment of Todd et al. experiments on Clasach sandstone cores (Todd et al. 1984): $\lambda_0=10$ 1/m, $\beta=100$, $\beta_2=-1,000$, and $\sigma_m=0.025$. Injected concentration $c^0=5$ ppm.

It follows from Eq. 12 that the larger the formation damage coefficient, the higher the impedance growth. The fourth “basic” curve with $\beta=100$ is located between Curves 1 and 5 that correspond to $\beta=150$ and $\beta=50$, respectively. In the basic case, Injectivity Index II decreases 2.8 times while for Cases 1 and 4 it decreases 4 and 1.6 times, respectively. The formation-damage coefficient β is the most influential parameter.

Increase in the second formation-damage coefficient from $\beta_2=-1,000$ to $\beta_2=0$ and further to $\beta_2=+1,000$ (Curves 3 and 2, respectively) results in some rise of the impedance curve.

The effect of filtration function on the impedance curve is exhibited in Fig. 9. The increase of initial filtration coefficient from $\lambda_0=5$ 1/m (Curve 4) to $\lambda_0=10$ 1/m and further to $\lambda_0=20$ 1/m (Curves 2 and 1, respectively) results in some impedance variation. Nevertheless, the difference between the curves disappears with time. This is explained by the fact that the limited value of impedance stabilization is not affected by λ_0 (i.e., it is determined by maximum retention concentration, and also by formation-damage coefficients that are equal for all curves in Fig. 9). Therefore, impedance Curves 1, 2, and 4 tend to the same limit.

The behavior of Curves 2, 3, and 5 corresponding to maximum retention concentrations $\sigma_m=0.025$, 0.015, and 0.0015, respectively, shows the sensitivity of impedance to σ_m variation. The larger the σ_m , the higher the impedance, including its limit value.

Summary

Four injectivity-damage coefficients for a deep-bed-filtration model with linear filtration and formation-damage functions can be determined from the pressure measurements in three points of a homogeneous core—at the core inlet, core outlet, and in some intermediate core point.

For four data sets of suspension corefloods, the parameters are obtained by adjustment of two pressure-drop curves for the overall core and for its first section, using the optimization technique. The proposed method validation was performed using the data of the laboratory tests, in which pressures have been measured in additional (fourth and fifth) core points. The predicted impedance curves for additional sections show good match with measured data for homogeneous artificial cores; a reasonably good match was observed for homogeneous natural outcrop core; a significant

deviation between the predicted and measured data was observed for natural heterogeneous cores.

The proposed method is valid for homogeneous cores. Additional work is required to investigate the sensitivity of the method with respect to core heterogeneity.

The well-injectivity index for the case of linear filtration and formation-damage functions decreases with time and stabilizes after long-time injection. The limit-injectivity value is independent of the filtration coefficient λ_0 . The formation-damage coefficient β is the most influential parameter for injectivity decline.

A similar method of complete characterization of the formation-damage system using pressure measurements with further prediction of well behavior can be applied for injection of poor-quality water, reinjection of produced water, drilling-fluid invasion into formation, migration of fines, and sulfate scaling (Tiab and Donaldson 1996; Bedrikovetsky et al. 2009; Civan 2007).

Nomenclature

- A = specific rock surface, L^2
- b = area on grain surface filled by one retained particle, L^2
- c = suspension particle concentration
- c^o = injected-suspension concentration
- h = formation thickness, L
- J = impedance
- k = permeability, L^2
- L = core length, L
- m = impedance slope
- p = pressure, M , T^{-2} , L^{-1}
- r = radius, L
- R_c = drainage (contour) radius, L
- t = time, T
- U = Darcy velocity, L , T^{-1}
- x = coordinate in linear geometry, L
- X = dimensionless coordinate in radial geometry
- β = formation-damage coefficient
- λ = filtration coefficient, L^{-1}
- λ_0 = value of filtration coefficient for $\sigma=0$, L^{-1}
- μ = viscosity of water, M , T^{-1} , L^{-1}
- σ = deposited-particles concentration
- ω = dimensionless length of first core
- ϕ = porosity

Superscripts and Subscripts

- 0 = initial
- D = dimensionless
- m = maximum
- w = well
- ω = dimensionless length of first core

Acknowledgments

Authors thank Petrobras for generous support of formation-damage projects during many years. Many thanks are owed to P. Currie (Delft University of Technology, the Netherlands) and Farid Shecaira and Alexandre Guedes S. (Petrobras/CENPES) for fruitful discussions. Pavel Bedrikovetsky also thanks the Australian School of Petroleum (University of Adelaide) for a generous startup grant.

References

- Al-Abduwani, F.A.H. 2005. Internal filtration and external filter cake build-up in sandstones. PhD thesis, Delft University of Technology, Delft, The Netherlands.
- Al-Abduwani, F.A.H., Shirzadi, A., van den Broek, W.M.G.T., and Currie, P.K. 2005. Formation Damage vs. Solid Particles Deposition Profile During Laboratory-Simulated Produced-Water Reinjection. *SPE J.* **10** (2): 138–151. SPE-82235-PA. doi: 10.2118/82235-PA.
- Ali, M.A.J., Currie, P.K., and Salman, M.J. 2005. Measurement of the Particle Deposition Profile in Deep-Bed Filtration During Produced Water Re-Injection. Paper SPE 93056 presented at the SPE Middle

- East Oil and Gas Show and Conference, Bahrain, 12–15 March. doi: 10.2118/93056-MS.
- Ali, M.A.J., Currie, P.K., and Salman, M.J. 2007. Permeability Damage Due to Water Injection Containing Oil Droplets and Solid Particles at Residual Oil Saturation. Paper SPE 104608 presented at the SPE Middle East Oil and Gas Show and Conference, Bahrain, 11–14 March. doi: 10.2118/104608-MS.
- Ali, M.A.J., Currie, P.K., and Salman, M.J. 2009. The Effect of Residual Oil on Deep-Bed Filtration of Particles in Injection Water. *SPE Prod & Oper* **24** (1): 117–123. SPE-107619-PA. doi: 10.2118/107619-PA.
- Alvarez, A.C., Bedrikovetsky, P.G., Hime, G., Marchesin, A.O., Marchesin, D., and Rodríguez, J.R. 2006a. A fast inverse solver for the filtration function for flow of water with particles in porous media. *Inverse Problems* **22**: 69–88. doi: 10.1088/0266-5611/22/1/005.
- Alvarez, A.C., Hime, G., Marchesin, D., and Bedrikovetsky, P.G. 2006b. The inverse problem of determining the filtration function and permeability reduction in flow of water with particles in porous media. *Transport in Porous Media* **70** (1): 43–62. doi: 10.1007/s11242-006-9082-3.
- Bachman, R.C., Harding, T.G., Settari, A., and Walters, D.A. 2003. Coupled Simulation of Reservoir Flow, Geomechanics, and Formation Plugging With Application to High-Rate Produced Water Reinjection. Paper SPE 79695 presented at the SPE Reservoir Symposium, Houston, 3–5 February. doi: 10.2118/79695-MS.
- Bailey, L., Boek, E.S., Jacques, S.D.M., Boassen, T., Selle, O.M., Argillier, J.F., and Longeron, D.G. 2000. Particulate Invasion From Drilling Fluids. *SPE J.* **5** (4): 412–419. SPE-67853-PA. doi: 10.2118/67853-PA.
- Bedrikovetsky, P., Marchesin, D., Shecaira, F., Souza, A.L., Milanez, P.V., and Rezende, E. 2001. Characterization of deep bed filtration system from laboratory pressure drop measurements. *J. Pet. Sci. Eng.* **32** (2–4): 167–177. doi: 10.1016/S0920-4105(01)00159-0.
- Bedrikovetsky, P.G. 1993. *Mathematical Theory of Oil and Gas Recovery: With Applications to ex-USSR Oil and Gas Fields*, Vol. 4, ed. G. Rowan, trans. R. Loshak. Dordrecht, The Netherlands: Petroleum Engineering and Development Studies, Kluwer Academic Publishers.
- Bedrikovetsky, P. 2008. Upscaling of Stochastic Micro Model for Suspension Transport in Porous Media. *Transport in Porous Media* **75** (3): 335–369. doi: 10.1007/s11242-008-9228-6.
- Bedrikovetsky, P., Tran, T.L., van den Broek, W.M.G.T., Marchesin, D., Rezende, E., Siqueira, A.G., Souza, A.L.S., and Shecaira, F.S. 2003. Damage Characterization of Deep-Bed Filtration From Pressure Measurements. *SPE Prod & Fac* **18** (2): 119–128. SPE-83673-PA. doi: 10.2118/83673-PA.
- Bedrikovetsky, P.G., Mackay, E.J., Silva, M.P., Patricio, F.M.R., and Rosário, F.F. 2009. Produced water re-injection with seawater treated by sulphate reduction plant: Injectivity decline, analytical model. *J. Pet. Sci. Eng.* **68** (1–2): 19–28. doi: 10.1016/j.petrol.2009.05.015.
- Chauveteau, G., Nabzar, L., and Coste, J.-P. 1998. Physics and Modeling of Permeability Damage Induced by Particle Deposition. Paper SPE 39463 presented at the SPE Formation Damage Control Conference, Lafayette, Louisiana, USA, 18–19 February. doi: 10.2118/39463-MS.
- Civan, F. 2007. *Reservoir Formation Damage: Fundamentals, Modeling, Assessment, and Mitigation*, second edition. Houston: Gulf Publishing Company.
- Harding, T.G., Norris, B., and Smith, K.H. 2002. Horizontal Water Disposal Well Performance in a High Porosity and Permeability Reservoir. Paper SPE 79007 presented at the SPE International Thermal Operations and Heavy Oil Symposium and International Well Technology Conference, Calgary, 4–7 November. doi: 10.2118/79007-MS.
- Harding, T.G., Varner, J., Flexhaug, L.A., and Bennion, D.B. 2003. Design and Performance of a Water Disposal Well Stimulation Treatment in a High Porosity and Permeability Sand. Paper PETSOC 2003-208 presented at the Canadian International Petroleum Conference, Calgary, 10–12 June. doi: 10.2118/2003-208.
- Herzig, J.P., Leclerc, D.M., and Goff, P.L. 1970. Flow of Suspensions through Porous Media—Application to Deep Filtration. *Ind. Eng. Chem.* **62** (5): 8–35. doi: 10.1021/ie50725a003.
- Miranda, R.M. and Underdown, D.R. 1993. Laboratory Measurement of Critical Rate: A Novel Approach for Quantifying Fines Migration Problems. Paper SPE 25432 presented at the SPE Production Operations Symposium, Oklahoma City, Oklahoma, USA, 21–23 March. doi: 10.2118/25432-MS.

- Moghadas, J., Müller-Steinhagen, H., Jamialahmadi, M., and Sharif, A. 2004. Theoretical and experimental study of particle movement and deposition in porous media during water injection. *J. Pet. Sci. Eng.* **43** (3–4): 163–181. doi: 10.1016/j.petrol.2004.01.005.
- Mojarad, R.S. and Settari, A. 2005. Multidimensional Velocity-Based Model of Formation Permeability Damage: Validation, Damage Characterization, and Field Application. Paper SPE 97169 presented at the SPE Annual Technical Conference and Exhibition, Dallas, 9–12 October. doi: 10.2118/97169-MS.
- Nabzar, L., Chauveteau, G., and Roque, C. 1996. A New Model for Formation Damage by Particle Retention. Paper SPE 31119 presented at the SPE Formation Damage Control Conference, Lafayette, Louisiana, USA, 14–15 February. doi: 10.2118/31119-MS.
- Nabzar, L., Aguilera, M.E., and Rajoub, Y. 2005. Experimental Study on Asphaltene-Induced Formation Damage. Paper SPE 93062 presented at the SPE International Symposium Oilfield Chemistry, The Woodlands, Texas, USA, 2–4 February. doi: 10.2118/93062-MS.
- Pang, S. and Sharma, M.M. 1997. A Model for Predicting Injectivity Decline in Water-Injection Wells. *SPE Form Eval* **12** (3): 194–201. SPE-28489-PA. doi: 10.2118/28489-PA.
- Rousseau, D., Hadi, L., and Nabzar, L. 2007. PWRI-Induced Injectivity Decline: New Insights on In-Depth Particle Deposition Mechanisms. Paper SPE 107666 presented at the European Formation Damage Conference, Sheveningen, The Netherlands, 30 May–1 June.
- Settari, A. 1985. A New General Model of Fluid Loss in Hydraulic Fracturing. *SPE J.* **25** (4): 491–501. SPE-11625-PA. doi: 10.2118/11625-PA.
- Sharma, M.M. and Yortsos, Y.C. 1987. Transport of particulate suspensions in porous media: Model formulation. *AIChE J.* **33** (10): 1636–1643. doi: 10.1002/aic.690331007.
- Soo, H., Williams, M.C., and Radke, C.J. 1986a. A filtration model for the flow of dilute stable emulsions in porous media—II. Parameter evaluation and estimation. *Chemical Engineering Science* **41** (2): 273–281. doi: 10.1016/0009-2509(86)87008-7.
- Soo, H. and Radke, C.J. 1986b. A filtration model for the flow of dilute stable emulsions in porous media—I. Theory. *Chemical Engineering Science* **41** (2): 263–272. doi: 10.1016/0009-2509(86)87007-5.
- Suryanarayana, P.V.R., Wu, Z., and Ramalho, J. 2007. Dynamic Modeling of Invasion Damage and Impact on Production in Horizontal Wells. *SPE Res Eval & Eng* **10** (4): 348–358. SPE-95861-PA. doi: 10.2118/95861-PA.
- Tang, Y., Yildiz, T., Ozkan, E., and Kelkar, M. 2005. Effects of Formation Damage and High-Velocity Flow on the Productivity of Perforated Horizontal Wells. *SPE Res Eval & Eng* **8** (4): 315–324. SPE-77534-PA. doi: 10.2118/77534-PA.
- Tiab, D. and Donaldson, E.C. 1996. *Petrophysics: Theory and Practice of Measuring Reservoir Rock and Fluid Transport Properties*, 706. Houston: Gulf Publishing Company.
- Todd, A.C., Noorkami, M., and Tweedie, J.A. 1979. Review of Permeability Damage Studies and Related North Sea Water Injection. Paper SPE 7883 presented at the SPE Oilfield and Geothermal Chemistry Symposium, Houston, 22–24. doi: 10.2118/7883-MS.
- Todd, A.C., Somerville, J.E., and Scott, G. 1984. The Application of Depth of Formation Damage Measurements in Predicting Water Injectivity Decline. Paper SPE 12498 presented at the SPE Formation Damage Control Symposium, Bakersfield, California, USA, 13–14 February. doi: 10.2118/12498-MS.
- van Oort, E., van Velzen, J.F.G., and Leerlooijer, K. 1993. Impairment by Suspended Solids Invasion: Testing and Prediction. *SPE Prod & Fac* **8** (3): 178–184; *Trans.*, AIME, **295**. SPE-23822-PA. doi: 10.2118/23822-PA.
- Wennberg, K.E. and Sharma, M.M. 1997. Determination of the Filtration Coefficient and the Transition Time for Water Injection. Paper SPE 38181 presented at the SPE European Formation Damage Conference, The Hague, 2–3 June. doi: 10.2118/38181-MS.
- Zang, L. and Dusseault, M.B. 2004. Sand-Production Simulation in Heavy-Oil Reservoirs. *SPE Res Eval & Eng* **7** (6): 399–407. SPE-89037-PA. doi: 10.2118/89037-PA.

Appendix A—Analytical Solution for Deep-Bed Filtration With Constant Injectivity Damage Coefficients

Consider the deep-bed-filtration system (Eqs. 1 and 3) with constant filtration coefficient. The solution of a so-called clean-bed

injection problem with zero initial conditions is well known—the detailed derivations can be found in Pang and Sharma (1997), Chauveteau et al. (1998), and Herzig et al. (1970). The solution is obtained by applying the method of characteristics to a linear system (Eqs. 1 and 3) with $\lambda = \text{const}$.

$$c(x, t) = \begin{cases} c^0 e^{-\lambda_0 x}, & x < Ut/\phi \\ 0, & x > Ut/\phi \end{cases}, \dots\dots\dots (\text{A-1})$$

$$\sigma(x, t) = \begin{cases} \lambda_0 c^0 (Ut - \phi x) e^{-\lambda_0 x}, & x < Ut/\phi \\ 0, & x > Ut/\phi \end{cases}, \dots\dots\dots (\text{A-2})$$

Because $x < L$, for long times $t \gg \phi L/U$ the second term in brackets in Eq. A-2 can be neglected if compared with the first term. Expressing pressure gradient from Eq. 5 and integrating it in x from zero to L yields the following expression for impedance:

$$J(t) = 1 + m \frac{Ut}{\phi L}, \dots\dots\dots (\text{A-3})$$

where the proportionality coefficient m is expressed by means of the filtration and formation-damage coefficients

$$m = \beta \phi c^0 (1 - e^{-\lambda_0 L}), \dots\dots\dots (\text{A-4})$$

Eq. A-4 is also valid for the first core section after substitution of L by ωL :

$$m_\omega = \beta \phi c^0 (1 - e^{-\lambda_0 \omega L}), \dots\dots\dots (\text{A-5})$$

Dividing Eq. A-5 by Eq. A-4 and introducing new unknown y ,

$$y = e^{-\lambda_0 L}, \dots\dots\dots (\text{A-6})$$

allows elimination of unknown β and yields the following transcendental equation:

$$y^\omega = \left(1 - \frac{m_\omega}{m}\right) + \frac{m_\omega}{m} y, \dots\dots\dots (\text{A-7})$$

The resulting Eq. A-7 allows determination of y and, consequently, calculation of filtration coefficient λ from measured constants m and m_ω (Bedrikovetsky et al. 2001, 2003).

Appendix B—Semianalytical Model for Axisymmetric Deep-Bed Filtration With Linear Damage Coefficients

The governing system for axisymmetric deep-bed filtration consists of equations for mass balance of suspended and retained particles,

$$\phi \frac{\partial c}{\partial t} + \frac{q}{2\pi rh} \frac{\partial c}{\partial r} = -\frac{\partial \sigma}{\partial t}, \dots\dots\dots (\text{B-1})$$

for kinetics of particle retention,

$$\frac{\partial \sigma}{\partial t} = \lambda_0 \left(1 - \frac{\sigma}{\sigma_m}\right) c \frac{q}{2\pi rh}, \dots\dots\dots (\text{B-2})$$

and for Darcy's law accounting for permeability damage,

$$\frac{q}{2\pi rh} = -\frac{k_0}{(1 + \beta\sigma + \beta_2\sigma^2)\mu} \frac{\partial p}{\partial r}, \dots\dots\dots (\text{B-3})$$

Exact analytical solution of a deep-bed-filtration system at linear geometry (Eqs. 1 and 3) was obtained by introduction of σ -dependent potential and by using the method of characteristics (Herzig et al. 1970; Soo et al. 1986a; Alvarez et al. 2006a, 2006b). Let us apply the potential function technique to the axisymmetric system (Eqs. B-1 and B-2). Introduce potential from Eq. B-2 as

$$c = -\frac{\partial}{\partial t} \left[\frac{2\pi rh \sigma_m}{\lambda_0 q} \ln(\sigma_m - \sigma) \right], \dots\dots\dots (\text{B-4})$$

substitute it into Eq. B-1, and integrate the result in t accounting for initial conditions $c(r, 0) = \sigma(r, 0) = 0$:

$$\frac{2\pi rh}{q} \frac{\partial \ln(\sigma_m - \sigma)}{\partial t} + \frac{\partial \ln(\sigma_m - \sigma)}{\partial r} = \frac{\lambda_0 \sigma}{\sigma_m} - \frac{\ln(\sigma_m - \sigma)}{r} + \frac{\ln(\sigma_m)}{r} \quad \dots \dots \dots (B-5)$$

Substituting the boundary condition $r=r_w$ and $c=c^0$ into Eq. B-4, we obtain the expression for the retention-concentration growth on the injector wall (sandface):

$$\sigma(r_w, t') = \sigma_m \left[1 - \exp \left(-\frac{\lambda_0 q c^0}{2\pi r_w h \sigma_m} t' \right) \right] \quad \dots \dots \dots (B-6)$$

Introduction of dimensionless coordinate and time t_D (as expressed in PVI),

$$t_D = \frac{qt}{\pi h R_c^2 \phi}, X = \left(\frac{r}{R_c} \right)^2, \quad \dots \dots \dots (B-7)$$

and applying the method of characteristics to the first-order partial-differential equation (Eq. B-5) subject to boundary condition Eq. B-6 yields the following Cauchy problem for an ordinary-differential equation:

$$\frac{d\sigma}{dX} = (\sigma_m - \sigma) \left[\frac{1}{2X} \ln \left(\frac{\sigma_m - \sigma}{\sigma_m} \right) - \frac{\lambda_0 R_c \sigma}{2\sqrt{X} \sigma_m} \right] \quad \dots \dots \dots (B-8)$$

$$X = X_w : \sigma = \sigma_m \left\{ 1 - \exp \left[\frac{\lambda_0 R_c c^0 \phi}{2\sqrt{X_w} \sigma_m} (t_D - X + X_w) \right] \right\} \quad \dots \dots (B-9)$$

The solution $\sigma(X, t_D)$ of the problem (Eqs. B-8 and B-9) is obtained by the Runge-Kutta method.

The well impedance (Eq. 9) is obtained from (Eq. B-3) by numerical integration in X for retained-concentration distribution $\sigma(X, t_D)$ as calculated by (Eqs. B-8 and B-9):

$$J(t_D) = -\frac{1}{\ln X_w X_w} \int_{X_w}^1 \frac{1 + \beta \sigma(X, t_D) + \beta_2 \sigma^2(X, t_D)}{X} dX \quad \dots \dots (B-10)$$

Pavel Bedrikovetsky holds an MSc degree in applied mathematics, a PhD degree in fluid mechanics, and a DSc degree in reservoir engineering from Moscow Oil-Gas Gubkin University. E-mail: pavel@asp.adelaide.edu.au. His research covers formation damage and IOR. Currently, Bedrikovetsky is a professor of petroleum engineering at the Australian School of Petroleum at the University of Adelaide. He served as Section Chairman, short course instructor, key speaker, and Steering Committee member at several SPE Conferences. Bedrikovetsky was a 2008–2009 SPE Distinguished Lecturer. **Alexandre Servulo Vaz Jr.** is a senior researcher in the petroleum department of the University of North Fluminense in Rio de Janeiro. He holds a PhD degree from the University of North Fluminense and an MSc degree from Federal University of Rio de Janeiro. His research and teaching interests cover formation damage and EOR. **Antonio Luiz Serra de Souza** is a senior petroleum engineer and consultant at Petrobras Research Center (CENPES) in Rio de Janeiro. de Souza is the coordinator of the research program for geomechanical and water-injection optimization and has been working with reservoir engineering for more than 25 years. He previously worked at Petrobras headquarters in reservoir simulation and EOR and managed the reservoir simulation section of CENPES from 1989 to 1993. de Souza holds an MS degree in mechanical engineering from Pontific Catholic University in Brazil and a PhD degree in petroleum engineering from Stanford University. **Claudio Alves Furtado** is a chemical engineer. He holds a degree from the Federal University of Rio de Janeiro (UFRJ), a postgraduate degree in petroleum engineering from Pontifical Catholic University of Rio de Janeiro, and a MSc degree in chemical engineering from UFRJ. Furtado has worked at the research center of Petrobras as a petroleum chemist since 2001 in the water management group with emphasis at injectivity decline models and prediction, produced water reinjection, and water injection surveillance.